Soil Biology and Biochemistry 125 (2018) 300–308

Contents lists available at ScienceDirect

Soil Biology and Biochemistry

journal homepage: www.elsevier.com/locate/soilbio

Vulnerability of DNA hybridization in soils is due to Mg^{2+} ion induced DNA aggregation

Xiaofang Wang[a], Hyojin Kweon[b], Seokho Lee[c], Hyejin Shin[d], Beelee Chua[e], Mark R. Liles[f], Ming-kuo Lee[g], Ahjeong Son[b,*]

[a] Department of Civil Engineering, Auburn University, Auburn, AL, 36849, USA
[b] Department of Environmental Science and Engineering, Ewha Womans University, Seoul, 03760, Republic of Korea
[c] Department of Statistics, Hankuk University of Foreign Studies, Global Campus, Yongin-si, Gyeonggi-do, 17035, Republic of Korea
[d] Samsung Research, Seoul, 06765, Republic of Korea
[e] School of Electrical Engineering, Korea University, Seoul, 02841, Republic of Korea
[f] Department of Life Science, Auburn University, Auburn, AL, 36849, USA
[g] Department of Geology, Auburn University, Auburn, AL, 36849, USA

ARTICLE INFO

Keywords:
Magnesium (Mg^{2+}) ion
Gene quantification
DNA hybridization
NanoGene assay
Atomic force microscopy

ABSTRACT

The NanoGene assay is an inhibitor-resistant gene quantification assay based on magnetic bead and quantum dot nanoparticles. It employs a set of probe and signaling probe DNAs to capture target DNA via hybridization. Using simple DNA preparation that bypasses conventional DNA extraction, it was able to detect and quantify specific bacterial genes in environmental sample. In this study, the vulnerability of the NanoGene assay to the presence of various environmental factors was investigated. A total of 43 soil samples were inoculated with 10^9 CFU/mL of *Pseudomonas putida* prior to DNA isolation without purification. Subsequently, the NanoGene assay was performed for quantitative detection of *P. putida* with respect to 12 soil properties including pH, moisture, humic acids, organic matter, sand, silt, clay, cation exchange capability, sodium, potassium, magnesium, and calcium. Using multiple linear regression, the NanoGene assay was found to be particularly vulnerable to the presence of Mg^{2+}, which was selected as a major variable ($P = 0.001$). The vulnerability of the NanoGene assay to Mg^{2+} was further explored by atomic force microscopy, which indicated significant Mg^{2+}-mediated DNA aggregation. The inhibition of the NanoGene assay from some soil samples as a consequence of DNA aggregation could therefore be prevented by the use of Mg^{2+} chelators such as EDTA, enabling application of this method across diverse soil types.

1. Introduction

The NanoGene assay is a gene quantification assay that uses two DNA probes to capture target genomic DNAs via hybridization. The DNA probes are tethered with quantum dots (QDs) and magnetic beads. This allows the magnetic separation of the captured target genomic DNA prior to gene quantification via fluorescence measurement. The NanoGene assay has been shown to be resistant to a number of environmental inhibitors including humic acids (Kim and Son, 2010; Kim et al., 2011a, 2011b; Wang et al., 2013), reducing the need for genomic DNA (gDNA) purification. In other words, laborious and expensive DNA purification methods necessary for some molecular analyses could be substituted in the NanoGene analysis with simple DNA isolation processes such as sonication or ozonation (Lee et al., 2015a, 2015b; Wang et al., 2015). Using rapid and simple DNA isolation methods for samples with very high humic acid content (> 1 μg/mL), the NanoGene assay only showed partial inhibition of 20–40%; in contrast, for the same samples qPCR assays showed 100% inhibition (Kim et al., 2011a; Wang et al., 2013).

The inhibition resistance of the NanoGene assay means that it is amenable for *in situ* monitoring applications, especially for pathogenic bacteria and toxic algal bloom detection (Mitchell et al., 2014; Lee et al., 2018). A simple DNA extraction process, rinse cycle, magnetic separation as well as fluorescence measurement can be incorporated into portable systems with relative ease (Mitchell et al., 2014; Lim et al., 2017b). Its versatility has also allowed variants of the NanoGene assay to be used for airborne bacteria as well as environmental hormone detection (Lee et al., 2016, 2017; Lim et al., 2017b). However, as the list of NanoGene assay applications grows, it becomes increasingly necessary to further explore its susceptibility to environmental factors.

* Corresponding author. Department of Environmental Science and Engineering, Ewha Womans University, Seoul, 03760, Republic of Korea.
E-mail address: ason@ewha.ac.kr (A. Son).

https://doi.org/10.1016/j.soilbio.2018.08.003
Received 4 April 2018; Received in revised form 26 July 2018; Accepted 3 August 2018
Available online 08 August 2018
0038-0717/

In this study, we explored the effect of many different environmental factors, including pH, moisture, humic acids, organic matter, sand, silt, clay, cation exchange capability, sodium, potassium, magnesium, and calcium. Furthermore, we evaluate the impact of specific environmental factors that inhibit NanoGene assay performance (i.e. high levels of Mg^{2+}) on DNA structure.

2. Materials and methods

2.1. Bacterial strain and culture conditions

P. putida strain DSM 8368 (DSMZ; Braunschweig, Germany) was used as a model bacteria as it is ubiquitous in the environment and often used for hydrocarbon bioremediation (Cébron et al., 2008). The freeze-dried culture of *P. putida* was revived in 1 mL of trypticase soy broth (TSB) at ambient temperature with a horizontal rotation at 160 rpm for 5 days, followed by growth on a trypticase soy agar plate at ambient temperature for 5 days. A single colony of *P. putida* was used to inoculate a 5 mL TSB culture and the optical density at 600 nm (OD_{600}) of culture was monitored each day using a SpectraMax M2 spectrofluorometer (Molecular Devices, Sunnyvale, CA, USA). When the OD_{600} reached 0.7 (*i.e.*, 10^9 CFU/mL), the bacterial culture was subjected to centrifugation at 5000 × *g* for 5 min and washed with cold 0.1 M phosphate buffered saline (pH 7.4) for 3 times to remove the residual broth. The washed culture was subjected to either spiking into soil samples or gDNA isolation in the following experiments.

2.2. Soil collection

Forty three soils were acquired from various locations in Alabama, Georgia, and Louisiana of the USA (Fig. 1). The recorded coordinates (altitude, latitude, and longitude) and the descriptions of the soil types are listed in Table S1. The soils were classified in eight categories: A. animal farms; B. vegetable farms; C. garden; D. forest; E. river sediment; F. lake sediment; G. marsh sediment; H. core sample. Soils from farms, forest, and garden were collected at 5–10 cm depth from the surface soil; the core samples were collected at 10–30 cm from the surface; the lake, river and marsh sediment were collected underneath the shallow water. All of the samples were sealed in plastic bags immediately after the collection and stored at −20 °C until further use.

2.3. Soil geochemical and physical properties

Each soil sample was characterized for 12 soil properties: pH, moisture (water content), organic matter (OM), humic acids (HA), sand, silt, clay, cation exchange capability (CEC), sodium ion (Na^+), potassium ion (K^+), magnesium ion (Mg^{2+}) and calcium ion (Ca^{2+}). The pH of the soil was determined using a pH meter with 1:5 ratio of soil and deionized water. The moisture of the samples was calculated by subtracting the original weight of the soil by the weight of the soil after the incubation in a 105 °C oven overnight and cooling down in a desiccator. The OM was determined by combusting the dry soils in the F62700 furnace (Barnstead International, Dubuque, IA) at 550 °C overnight, and cooling them down in the 105 °C oven followed by the desiccator. For the HA analysis, it was first extracted using acid/base alternation and the corresponding centrifugation since HA is soluble in basic condition and insoluble in acidic condition (Ting et al., 2010; Wang et al., 2013). Subsequently, the extracted HA was quantified by measuring the optical density at 320 nm (Wang et al., 2013). Other soil properties including soil texture, cations, and CEC were determined in the Auburn University Soil Testing Laboratory. The soil texture (*i.e.*, sand, silt, clay) was determined using a hydrometer method based on the sedimentation rate of particles in water. The concentration of cations (Na^+, K^+, Mg^{2+}, and Ca^{2+}) were determined by an inductively coupled plasma atomic emission spectrometer. Finally, CEC was determined with 1 M ammonium acetate based on the standard method of the Natural Resource Conservation Service (Burt, 2004).

2.4. Bacterial culture spiking and simple DNA isolation

A 500 µL aliquot of a *P. putida* TSB culture (~10^9 CFU/mL) was spiked into 500 mg of each soil sample in a 2 mL vial, and it was incubated overnight at ambient temperature to simulate the starvation of the cells in the environment. Since each soil sample may have contained indigenous *P. putida*, a duplicate soil sample without spiking *P. putida* was used as a negative control.

After incubating the bacterial cells in each soil sample overnight, gDNA was isolated by a simple physical lysis method as previously developed (Wang et al., 2015). The soil sample was resuspended with 1 mL of 0.1 M phosphate buffered saline (pH 7.4), and then sonicated using a XL-2000 ultrasonic dismembrator (Qsonica, Newtown, CT) with a 2 mm P-3 aluminum microprobe (Qsonica) at 10 W ultrasonication for 15 s on ice. The microprobe was cleaned with 70% ethanol between samples to prevent cross contamination. The soil and cell debris in the tubes were allowed to settle for 5 min, then 5 µL of the supernatant, which contains free DNA, was used for further gene quantification by the NanoGene assay. For a positive control, gDNA was isolated from the same amount of *P. putida* culture using the commercial DNA isolation kit (FastDNA® SPIN Kit for Soil, MP Biomedicals, Solon, OH).

2.5. NanoGene assay

The NanoGene assay uses a sandwich DNA hybridization and dual fluorescence system for gene quantification (Fig. 2a) (Kim and Son, 2010). First of all, 8 µL of 2 µM carboxyl QD_{565} (quantum dots, Life Technologies, Grand Island, NY) was immobilized on the surface of 100 µL of 2 × 10^8/mL aminated magnetic beads (MB, Dynabead® M-270, Life Technologies) with an aid of EDC (ethylcarbo-diimide hydrochloride) and NHS (N–hydroxysuccinimide). Subsequently, the probe DNA (5 µL, 100 nM) designed to be complementary to the target PAH-RHD_α gene was conjugated onto the QD_{565}, making the MB-QD-probe DNA complex a carrier of the NanoGene assay. The signaling part of the NanoGene assay was made up of the 8 µL of 2 µM QD_{655} covered with 1.6 µL of 100 nM signaling probe DNA, which was also designed to be complementary to the target PAH-RHD_α gene in *P. putida*.

The DNA hybridization was carried out in a 0.6 mL Eppendorf tube with both carrier and signaling parts in 400 µL hybridization buffer (Roche Diagnostic, Basel, Switzerland). Five µL aliquots of target DNA (lysed soil sample or gDNA) was added to the buffer and this was incubated in a hybridization oven (UVP HB-500 Minidizer Hybridization, Fisher Scientific) with a slow vertical rotation at 42 °C overnight.

After incubation, un-hybridized signaling probes with QD_{655} were removed by washing three times with phosphate buffer (0.1 M, pH = 7.4). The hybridized complex was then re-suspended in 200 µL of phosphate buffer and transferred to an opaque 96-well microplate (Nunc, Roskilde, Denmark) for endpoint fluorescence measurement using a SpectraMax M2 spectro-fluorometer. The emission wavelength for QD_{655} (*i.e.*, signaling fluorescence) and QD_{565} (*i.e.*, internal standard) was 655 nm and 565 nm, respectively, at 360 nm of photo-excitation. Subsequently, the normalized fluorescence (QD_{655}/QD_{565}) was used to determine % quantitative capability as shown in Eq. (1).

$$\textit{Quantitative Capability},\ \% = \frac{F_{sample} - F_{N.C.}}{F_{P.C.}} \times 100 \qquad \text{(Eq. 1)}$$

F_{sample} is the normalized fluorescence (QD_{655}/QD_{565}) of the NanoGene assay, which quantifies *P. putida* in each cell-spiked soil sample; $F_{N.C.}$ is the normalized fluorescence (QD_{655}/QD_{565}) of the NanoGene assay for the soil sample without cell spiking (negative control); $F_{P.C.}$ is the normalized fluorescence (QD_{655}/QD_{565}) of the NanoGene assay, which quantifies *P. putida* in the form of gDNA isolated by conventional gDNA isolation kit (positive control).

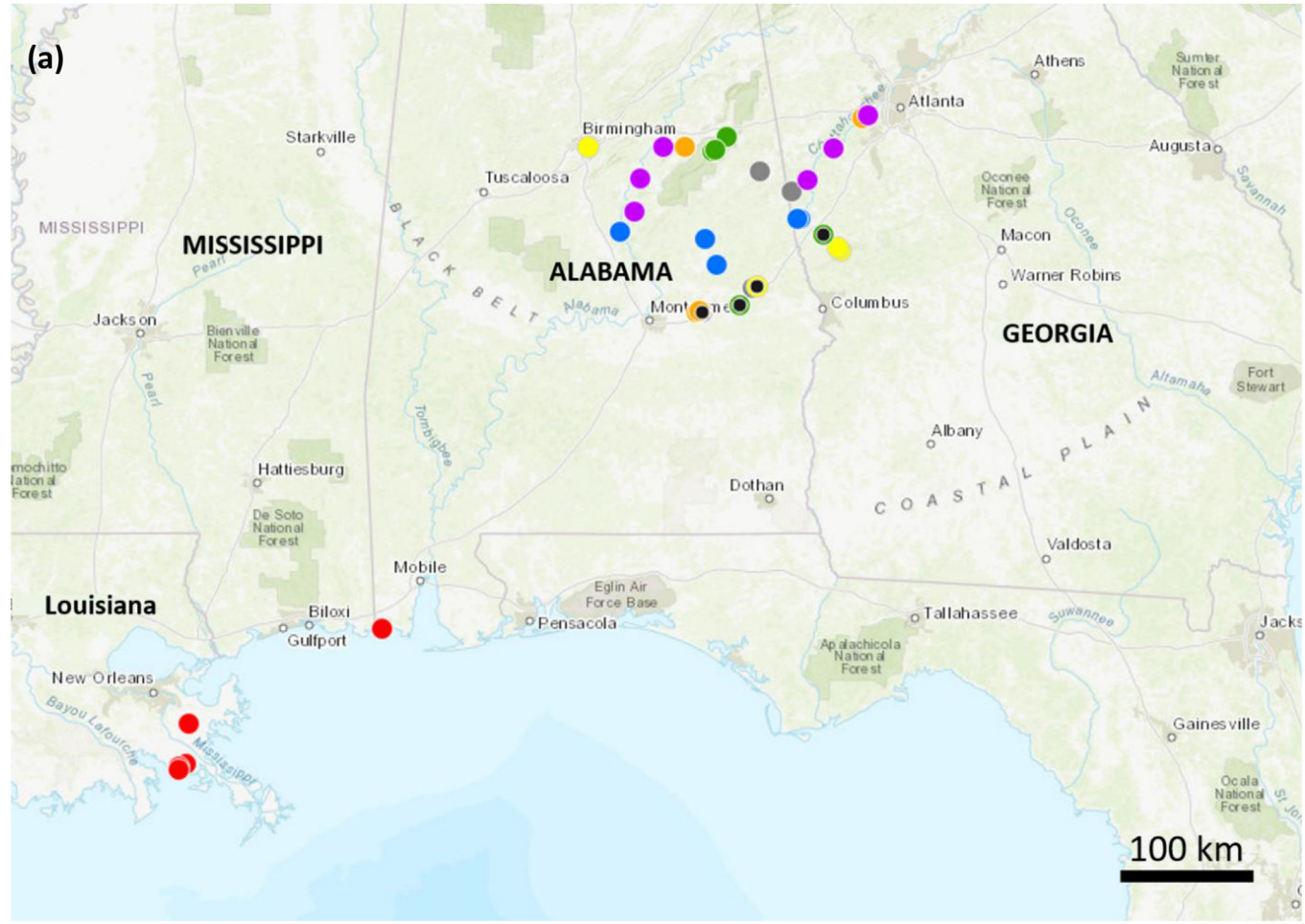

Fig. 1. (a) Geographical location of the sample collecting sites. Each color represent the soil categories of the sampling sites (gray: A. animal farms; orange: B. vegetable farms; yellow: C. gardens; green: D. forest; purple: E. river sediment; blue: F. lake sediment; red: G. marsh sediment; black: H. core samples). (b) Picture of sampled soils. (For interpretation of the references to color in this figure legend, the reader is referred to the Web version of this article.)

2.6. Statistical analysis

A multiple linear regression analysis was performed to derive an expression that relates the quantitative capability of NanoGene assay as affected by soil properties. As shown in Table 1 and Table S2, 11 explanatory (independent) variables (*i.e.*, pH, Moi, OM, HA, silt, clay, CEC, K^+, Na^+, Mg^{2+}, and Ca^{2+}) were tested against one response (dependent) variable (*i.e.*, quantitative capability of NanoGene assay) by implementing it to Eq. (2). Please note that the sand was omitted from the list of explanatory variables, since in the soil texture, the sum of sand, silt and clay is 100%.

$$y=\beta_0+\sum_{i=0}^{N}\beta_i x_i+\varepsilon \quad \text{(Eq. 2)}$$

Where y is the response variable, x is the explanatory variables, β_0 is the intercept of the model, β_i is the coefficient of the i th soil property, and ε is the random error.

In order to determine the significant variables that influenced the NanoGene quantitative capability, a number of variable selection techniques (total of 10 modeling methods) were performed: (1) lasso, elastic net, scad, mcp as regularization method, (2) adjusted R2,

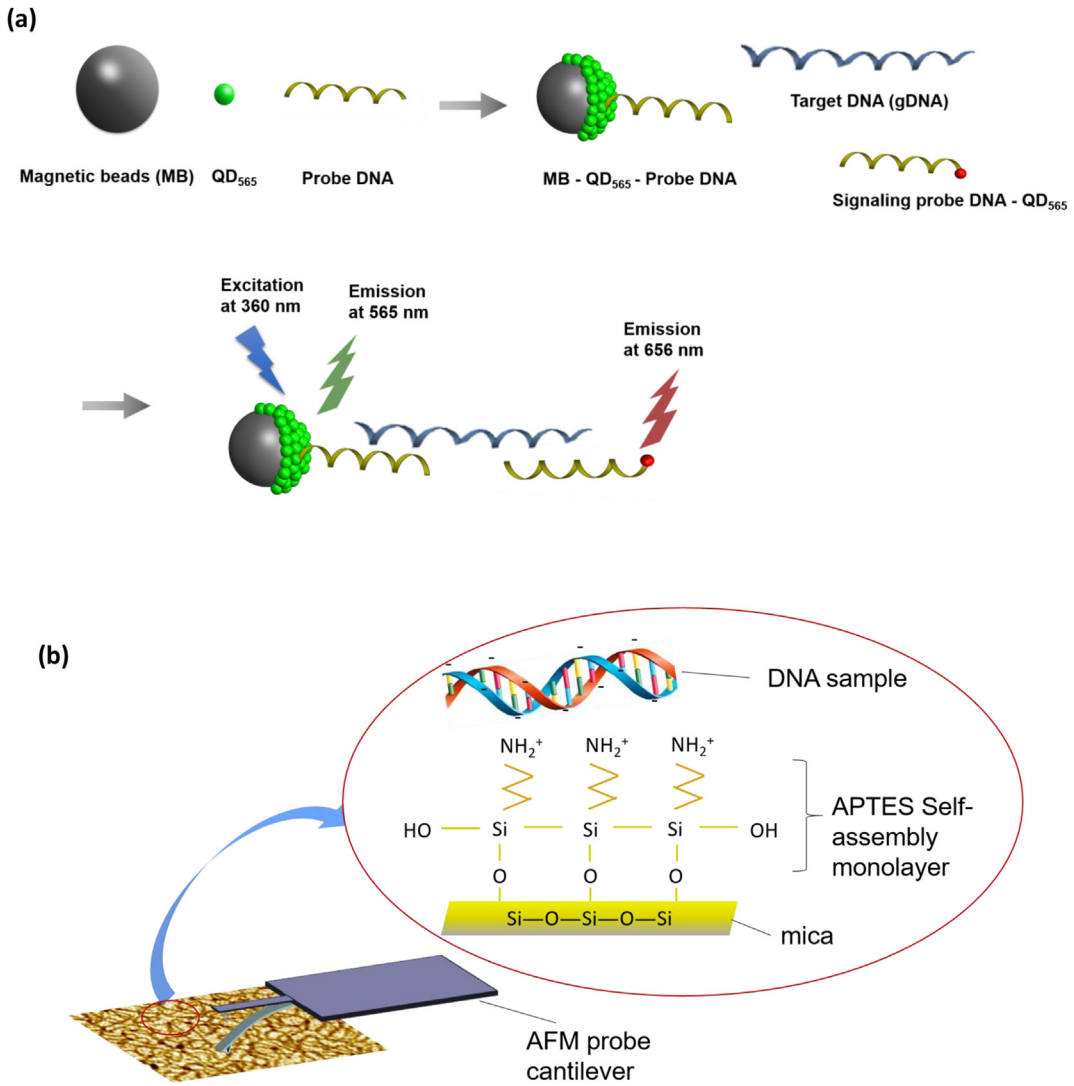

Fig. 2. (a) Schematics of gene quantification by the NanoGene assay. (b) Schematics of AFM imaging analysis.

Mallow's Cp, BIC as best subset selection, (3) forward, backward, stepwise as stepwise selection. Multiple linear regression and variable selections were performed by R software (version 3.4.3).

2.7. AFM imaging and zeta potential measurement

In order to observe the behavior of DNA in the presence of Mg^{2+} and HA, atomic force microscopy (AFM) imaging and zeta potential measurements were conducted.

2.7.1. DNA preparation

P. putida 16S rRNA gene PCR product was obtained to be used as a template for the AFM and zeta potential experiments. A *P. putida* TSB culture was used for gDNA isolation using a PowerSoil DNA Isolation kit (Qiagen, Germantown, MD). PCR was performed in an Applied Biosystems 2620 Thermal Cycler targeting a 16S rRNA gene amplicon (1465 bp) with the primer set of 27F (5′-AGA GTT TGA TCM TGG CTC AG-3′) and 1492R (5′-ACG GYT ACC TTG TTA CGA CTT-3′) and TaKaRa EX *Taq* polymerase. The temperature conditions for PCR amplification was 94 °C for 5 min; followed by 35 cycles consisting of 94 °C for 1 min, 55 °C for 1 min, and 72 °C for 2 min; a final cycle of 72 °C for 15 min. PCR products were purified using DNA Clean & Concentrator™-5 kit (Zymo, Irvine, CA). The quantity and purity of the DNA were determined using a NanoDrop™ 2000 Spectrophotometer (Thermo Fisher Scientific, Waltham, MA).

2.7.2. AFM imaging

The schematic diagram of AFM imaging is shown in Fig. 2b. PCR amplicons (5 μg/mL) were immobilized on the mica (ParkSystems, Suwon, Korea), which was functionalized by 3-aminopropyl-triethoxysilane (APTES, Sigma-Aldrich). Then 20 μL of 0.1% (v/v) APTES solution as a self-assembled monolayer was deposited on the freshly cleaved mica and incubated for 15 min under ambient environmental conditions. The excess APTES was rinsed with deionized water and the surface was air-dried. Subsequently, samples (5 μg/mL DNA control, 5 μg/mL DNA + 2 mM Mg^{2+}, 5 μg/mL DNA + 10 mM Mg^{2+}, 5 μg/mL DNA + 0.1 μg/mL HA, 5 μg/mL DNA + 0.5 μg/mL HA, 5 μg/mL DNA + 10 mM Mg^{2+} + 0.1 μg/mL HA, or 5 μg/mL DNA + 10 mM Mg^{2+} + 0.5 μg/mL HA) in 2 mM Tris-HCl buffer (pH 7.5) was deposited on APTES-mica for 15 min. Following rinsing with deionized water and air-drying, the sample was subjected to AFM imaging by Park NX10 (ParkSystems) with PPP-NCHR cantilever (Nanosensors™, Switzerland) of the force constant 42 N/m. HA as a form of Suwannee river standard was purchased from International humic substances society (IHSS) and it was diluted to 0.1 and 0.5 μg/mL of working concentration. Mg^{2+} solution as 2 and 10 mM of working concentrations was prepared from $MgCl_2{\cdot}6H_2O$ (Daejung, Korea).

Table 1
Geochemical and physical soil properties and gene quantitative capability measured by the NanoGene assay.

No.	Categories	Sample ID	pH	Moisture (%)	Organic Content		Soil Texture			CEC (cmol/kg)	K^+ (mg/kg)	Na^+ (mg/kg)	Mg^{2+} (mg/kg)	Ca^{2+} (mg/kg)	QC (%)
					Organic Matter (%)	Humic Acids (μg/mL)	Sand (%)	Silt (%)	Clay (%)						
1	A: Animal	A1	6.85	15	2	109	51	39	10	6	123	5	257	790	29
2	Farms	A2	7.44	8	3	33	64	26	10	8	89	30	253	1030	0
3		A3	6.94	12	2	125	68	27	5	4	56	12	36	739	48
4		A4	7.16	17	3	58	64	24	12	7	65	13	153	1113	70
5		A5	4.92	20	1	2	49	29	22	2	47	12	40	25	52
6	B: Vegetable	B1	5.32	9	2	426	61	29	10	6	252	8	46	248	18
7	Farms	B2	7.79	7	1	32	75	20	5	6	93	4	281	713	14
8		B3	7.10	11	3	269	42	53	5	10	105	10	35	1853	49
9		B4	7.48	24	6	51	43	50	8	18	378	19	184	3142	35
10		B5	6.71	26	5	254	56	42	2	10	216	5	203	1559	34
11	C: Garden	C1	5.34	26	8	754	73	24	3	8	116	15	94	601	37
12		C2	6.39	20	4	81	86	14	0	8	151	7	241	755	37
13		C3	7.47	27	17	64	54	43	4	29	136	21	579	4711	17
14		C4	5.92	22	5	427	47	48	5	12	99	17	168	1159	31
15		C5	4.93	15	2	192	74	24	3	3	105	4	24	2	45
16	D: Forest	D1	5.51	8	2	299	89	11	0	4	71	4	40	219	42
17		D2	5.46	6	2	222	86	11	3	2	57	6	18	47	76
18		D3	5.22	11	3	81	71	16	13	3	61	4	50	92	66
19		D4	6.78	23	8	349	46	52	2	13	175	36	397	1906	34
20		D5	7.88	18	8	149	54	43	4	21	104	18	81	4039	32
21		D6	4.83	16	3	361	56	39	5	4	57	16	65	70	47
22	E: River	E1	5.86	38	5	611	44	51	6	15	178	23	244	1650	19
23	Sediment	E2	7.82	21	3	7	51	39	9	12	42	40	112	2183	46
24		E3	7.16	31	1	25	85	12	3	4	41	18	78	646	37
25		E4	6.47	18	1	93	74	26	0	2	43	19	59	356	27
26		E5	6.92	54	9	215	52	45	3	7	168	42	136	1081	29
27		E6	5.26	22	2	152	74	23	4	3	57	16	37	224	14
28		E7	6.82	38	4	144	64	34	2	5	111	23	93	797	21
29	F: Lake	F1	7.24	22	0	1	98	2	1	1	50	9	27	97	60
30	Sediment	F2	5.80	21	2	29	32	42	26	5	76	11	88	354	70
31		F3	5.51	31	2	1	29	31	39	4	103	20	136	231	81
32		F4	5.47	14	1	6	62	21	18	2	64	16	70	71	47
33		F5	5.43	26	3	136	43	26	31	4	71	18	66	210	58
34	G: Marsh	G1	7.73	50	9	200	1	30	69	11	121	1685	165	254	32
35	Sediment	G2	7.81	49	9	210	1	20	79	12	109	1700	175	215	41
36		G3	7.00	48	9	192	1	25	76	12	133	1695	156	225	33
37		G4	6.60	47	10	205	1	22	77	10	103	1540	163	235	33
38		G5	7.20	52	10	215	1	32	67	11	113	1680	142	262	44
39	H: Core	H1	6.92	13	2	99	56	34	10	5	101	4	201	609	19
40	Sample	H2	4.92	9	2	242	86	11	3	2	69	2	16	24	30
41		H3	5.13	7	1	174	84	13	4	2	69	4	10	0	95
42		H4	4.88	18	6	97	68	21	12	2	39	3	27	29	100
43		H5	6.00	16	4	404	63	14	3	8	140	5	115	120	24

2.7.3. Zeta potential

Zeta potential measurements were performed by laser Doppler velocimetry using the zeta potential analyzer ELSZ-2000 (Otsuka Electronics, Osaka, Japan). The zeta potential (ζ) of four samples (5 μg/mL DNA, 5 μg/mL DNA + 10 mM Mg^{2+}, 5 μg/mL DNA + 0.1 μg/mL HA, or 5 μg/mL DNA + 10 mM Mg^{2+} + 0.1 μg/mL HA) was measured. These four samples are identical to the samples shown in Fig. 4a, c, 4d, and 4f, respectively. Three mL of the sample were transferred to the Otsuka zeta flow cells and measured. Zeta potential measurement was carried out in triplicate with six measurements for each sample.

3. Results and discussion

3.1. Influence of soil properties on the quantitative detection of P. putida using the NanoGene assay

To investigate the effect of environmental factors on NanoGene assay capability, a number of environmental soils and soil properties were examined for *P. putida* detection. The results of 12 soil properties (*i.e.*, pH, moisture, HA, OM, sand, silt, clay, CEC, Na^+, K^+, Mg^{2+}, and Ca^{2+}) and the quantitative capability of the NanoGene assay of the 43 soil samples were presented in Table 1. All of the values of the soil properties are within the range of the national survey of the soil (Shacklette and Boerngen, 1984). Quantitative capability varied markedly with values ranging from 0 to 100%, which indicates the NanoGene assay was partially inhibited by soil materials since the DNA was extracted by simple cell lysis without extensive purification.

Table 2
Selection of major variables by a variety of modeling methods.

Selection methods	pH	Moi	OM	**HA**	Sand	Silt	Clay	CEC	K^+	Na^+	**Mg^{2+}**	Ca^{2+}
Lasso	✓			✓			✓		✓		✓	
Elastic net	✓			✓			✓		✓		✓	
SCAD				✓							✓	
MCP				✓							✓	
Adjusted R2		✓	✓	✓			✓	✓		✓	✓	
Mallow's Cp							✓			✓	✓	
BIC							✓			✓	✓	
Forward selection	✓		✓	✓							✓	
Backward elimination			✓	✓			✓			✓	✓	
Stepwise selection	✓		✓	✓							✓	
Frequency	4	1	4	**8**		0	6	1	2	4	**10**	0

The bold indicates two major soil properties that were selected by various modeling methods.

Multiple linear regression analysis was used to better describe the influences of soil properties on the quantitative detection of *P. putida* using the NanoGene assay. First of all, the result of multiple linear regression analysis using all 11 exploratory variables (*i.e.*, pH, moisture, HA, OM, silt, clay, CEC, Na^+, K^+, Mg^{2+}, and Ca^{2+}) is shown in Table S2. All 11 variables explain 45.4% ($R^2 = 0.454$) of data variability in quantitative capability of the NanoGene assay. The relationship describing quantitative capability using 11 soil properties is as follows:

$$\text{Quantitative Capability (\%)} = 60.192 - 0.831\ \text{pH} - 0.339\ \text{Moi} + 3.812\ \text{OM} - 0.022\ \text{HA} - 0.117\ \text{Silt} + 0.872\ \text{Clay} - 1.254\ \text{CEC} - 0.030\ K^+ - 0.038\ Na^+ - 0.094\ Mg^{2+} + 0.001\ Ca^{2+} \quad \text{(Eq. 3)}$$

Since the relationship between quantitative capability and 11 soil properties is quite complex and not significant (all *P* values in Table S2 were greater than 0.05), major soil properties were selected based on different modeling techniques (Table 2) to indicate significant influences on the quantitative capability of the NanoGene assay.

As a result of these analyses, Mg^{2+} and HA were identified as the major variables affecting NanoGene assay quantification of *P. putida* in soils. From the result of the 10 modeling methods used (Table 2), Mg^{2+} was identified as a significant variable all 10 times and HA was also identified in eight of the models. Interestingly, the abundance of clay was also indicated as a significant variable in six of the modeling methods. Since clay-rich soils such as marsh and lake sediment (Fig. S1, $R^2 = 0.91$) can have greater cation sorption capacity, the clay content is predicted to have a direct relationship with Mg^{2+} concentration and affect the NanoGene assay via that mechanism. The two explanatory variables (Mg^{2+}, HA) had a *P* value being less than 0.05 or marginal (Table 3), indicating that they were significant contributors to the prediction of the quantitative capability of the NanoGene assay in different soils. The multiple linear regression model demonstrating the relationship describing quantitative capability using two salient soil properties is as follows:

$$\text{Quantitative Capability (\%)} = 58.369 - 0.031\ \text{HA} - 0.089\ Mg^{2+} \quad \text{(Eq. 4)}$$

Table 3
Multiple linear regression result that relates two major selected soil properties (HA and Mg^{2+}) to quantitative capability of the NanoGene assay ($r^2 = 0.268$).

Variable	Description	*P* value of multiple linear regression	Estimated parameter	Standard error
(Intercept)	Intercept of multiple linear regression	< 0.0001	58.369	5.505
HA	Humic acids (μg/mL)	0.090	−0.031	0.018
Mg^{2+}	Magnesium ion (mg/kg)	0.001	−0.089	0.026

The model suggests that quantitative capability increased with decreasing Mg^{2+} and HA. The two variables explained 26.8% ($R^2 = 0.268$) of the variability in quantitative capability of the NanoGene assay, while all 11 variables together explained 45.4% ($R^2 = 0.454$) of the variability in quantitative capability.

3.2. Major soil properties affecting NanoGene quantitative capability

The two major soil properties (Mg^{2+} and HA) that significantly affected NanoGene detection of *P. putida* were further evaluated by plotting the concentration of HA or Mg^{2+} vs. the relative NanoGene quantitative capability (Fig. 3a and b). This revealed the relatively strong predictive power of Mg^{2+} relative to HA in determining NanoGene quantitative capability; for example, all of the soil samples (n = 9) that were determined to have > 200 mg/kg Mg^{2+} concentration had < 50% NanoGene detection of *P. putida.* Whereas with HA concentrations, the soil samples (n = 5) with > 400 μg/mL HA levels had < 50% NanoGene quantitative capability, but there were also many samples with poor NanoGene performance that had negligible HA levels (Fig. 3a and b).

The most significant soil property identified was the Mg^{2+} concentration in the soil (Table 3; $P = 0.001$), indicating that it had the most significant influence on the quantitative capability of the NanoGene assay. The inhibitory effect of Mg^{2+} on the quantitative capability of the NanoGene assay was hypothesized to be due to Mg^{2+} binding with DNA, forming a super molecular aggregated DNA structure. DNA aggregation may hinder the DNA denaturation and subsequent hybridization in the NanoGene assay, resulting in reduced quantitative capability. Interestingly, the inhibitory effect of Ca^{2+} was negligible despite observations that Ca^{2+} levels in some soil samples was abundant (Table 1). However, Ca^{2+} was not selected as a variable affecting NanoGene detection in any of the modeling methods (Table 2). A potential explanation for the lack of an effect of Ca^{2+} on the NanoGene assay would be the larger ionic radius for Ca^{2+} that may not hinder DNA binding compared to Mg^{2+}.

In contrast to Mg^{2+}, the effect of HA on NanoGene quantitative capability was marginal (Table 3; $P = 0.09$). Based on a linear regression ($r^2 = 0.054$), it was difficult to define a linear relationship between HA and QC (Fig. 3b). HA is known as one of the major inhibitors in the environment for PCR-based assays because of its inhibition of *Taq* polymerase (Tebbe and Vahjen, 1993). However, the inhibitory effect of HA on *P. putida* detection with the NanoGene assay was not significant.

The concentration of Mg^{2+} in soils across eight different soil categories (Table 1) was evaluated (Fig. 3c). Two soil types with the lowest levels of Mg^{2+} were lake sediments (F, 77.4 mg/kg ± 39.6) and core samples (H, 73.8 mg/kg ± 82.9), both of which had the highest average NanoGene quantitative capabilities of 63.1% ± 12.6 and 53.8% ± 40.2, respectively (Fig. 3c and d, see arrows). Due to a large degree of variability among soil samples, these results were not

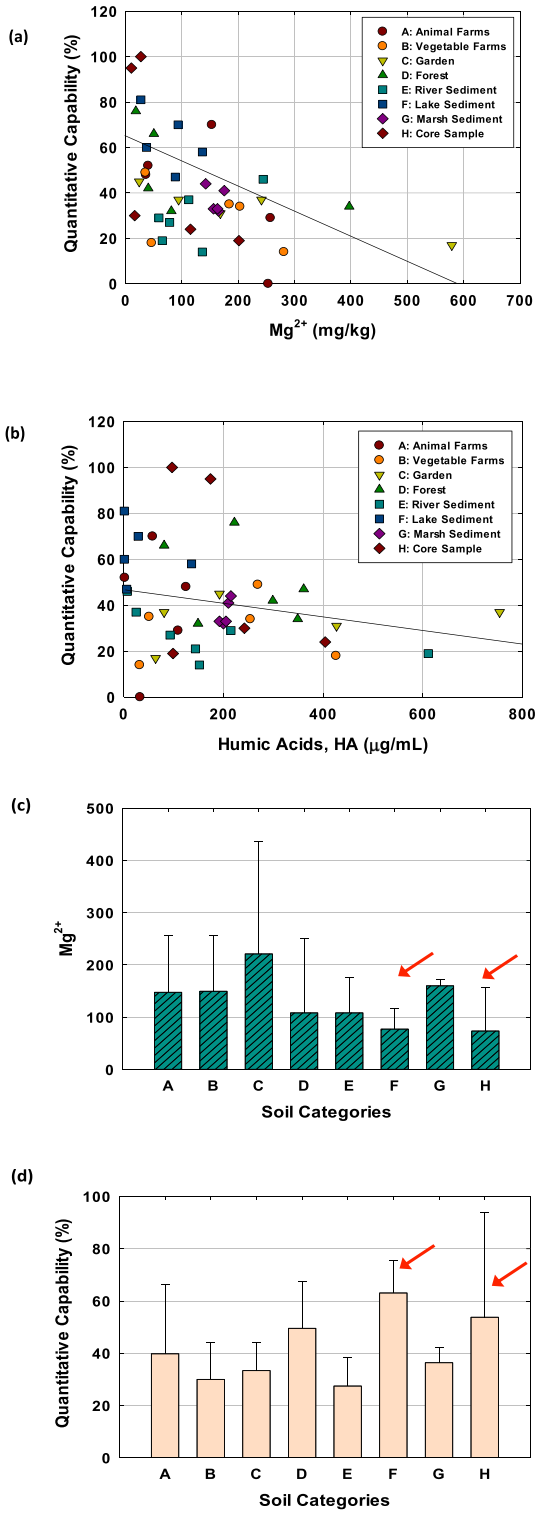

Fig. 3. (a) (b) Relationship between the quantitative capability of the NanoGene assay and major soil properties: Mg^{2+} and HA, respectively. Lines in (a) (b) refer to linear regression line (r^2 = 0.213 and 0.054 for Mg^{2+} and HA, respectively). (c) Mg^{2+} per each soil category. (d) Quantitative capability per each soil category. The bars and the errors in (c)–(d) represent the mean and the standard deviation of values in the each category (A: Animal Farms, B: Vegetable Farms, C: Garden, D: Forest, E: River Sediment, F: Lake Sediment, G: Marsh Sediment, H: Core Sample). Arrows in (c)–(d) refer to F (Lake Sediment) and H (Core Sample) that have shown the lowest levels of Mg^{2+} and highest average NanoGene quantitative capabilities.

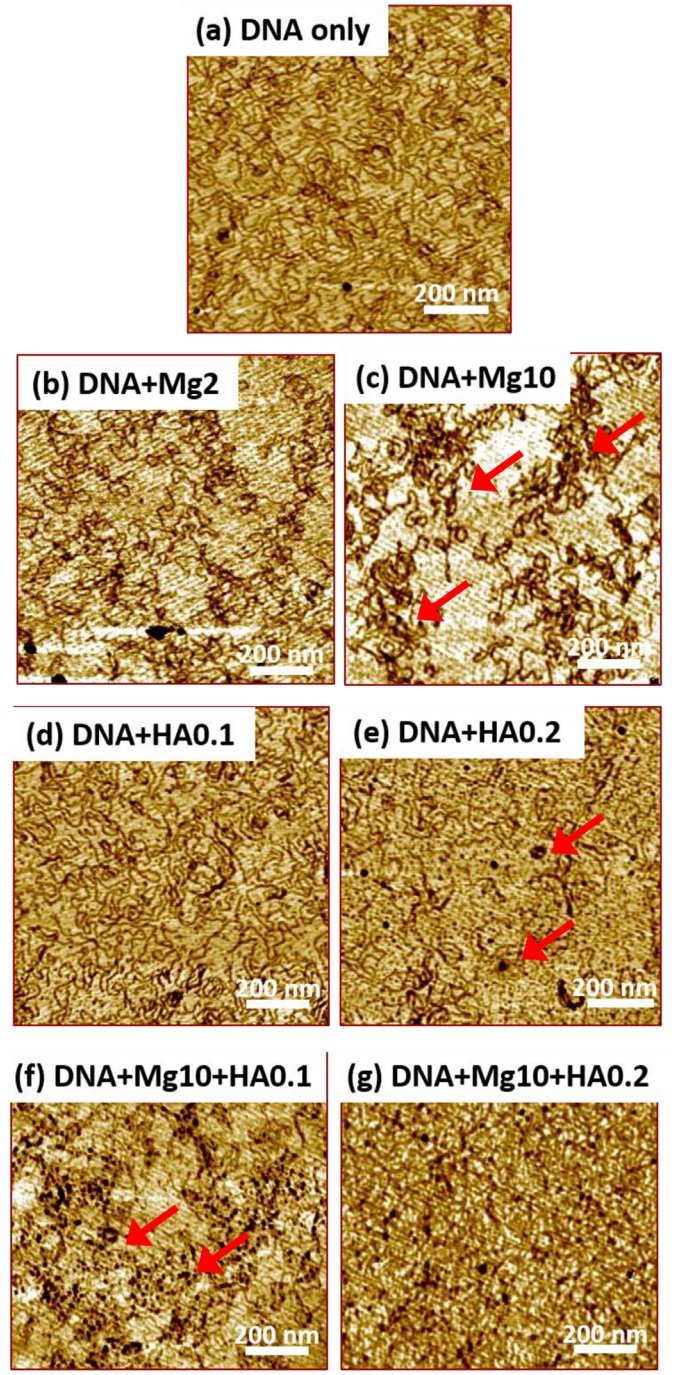

Fig. 4. AFM topographical images (1 μm × 1 μm) showing the DNA behavior in the presence of Mg^{2+} and/or HA. (a) DNA only: a negative control containing DNA only (PCR amplicon 5 μg/mL). The same concentration of DNA was used (b) through (g). Control DNA sample is used for identifying the change of DNA behavior by the presence of Mg^{2+} and/or HA in (b)–(g). (b) (c) DNA + Mg2 and DNA + Mg10 refer to DNA with Mg^{2+} 2 mM and 10 mM, respectively. (d) (e) DNA + HA0.1 and DNA + HA0.2 refer to DNA with HA 0.1 μg/mL and 0.5 μg/mL, respectively. (f) (g) DNA + Mg10 + HA0.1 or DNA + Mg10 + HA0.2 refer to DNA with Mg^{2+} 10 mM and HA 0.1 μg/mL or 0.5 μg/mL, respectively. The arrows in Figure 4c indicate the DNA aggregation induced by the presence of Mg^{2+} ions. The arrows in Figure 4e and f indicate the possible existence of HA as shown in darker dots.

significantly different to other soil samples. Nevertheless, these two soil types were noted for their lower Mg^{2+} levels and concomitant improved NanoGene assay performance.

Table 4
Zeta potential measurement for DNA with Mg^{2+} and HA. The results were obtained from triplicate samples with the six measurements for each sample.

Sample	Zeta potential (mV)
DNA only	−49.98 ± 3.18
DNA + Mg^{2+}	−17.20 ± 2.99
DNA + HA	−49.68 ± 1.41
DNA + Mg^{2+} + HA	−14.91 ± 4.69

3.3. Behavior of DNA in the presence of Mg^{2+} and HA

AFM imaging (Fig. 4) and zeta potential analysis (Table 4) were performed to further observe the behavior of DNA in the presence of Mg^{2+} and/or HA.

A well dispersed DNA structure was observed for the *P. putida* 16S rRNA gene PCR product by AFM, in both images of 1 μm × 1 μm (Fig. 4a) and 5 μm × 5 μm (SI, Fig. S2a) without any evidence of DNA aggregation. The zeta potential result of the control DNA sample (DNA only) was −49.98 ± 3.18 mV (Table 4). This zeta potential result indicates that DNA without any Mg^{2+} or HA has a stable dispersion since the surface charge values of > ± 30 mV indicate well dispersed particles (colloids) with no aggregation (ASTM, 1985).

Interestingly but not surprisingly, DNA with Mg^{2+} ions showed a dramatic change of DNA structure as compared to control DNA (Fig. 4b and c). In the presence of 2 mM or 10 mM Mg^{2+}, locally clustered DNA strands were observed that indicated strong DNA aggregation. At 10 mM Mg^{2+}, the observed DNA aggregation was stronger (Fig. 4c, see arrows). At the same time, the zeta potential of DNA with 10 mM Mg^{2+} ion was reduced to −17.20 ± 2.99 mV from −49.98 ± 3.18 mV observed for the DNA control, further indicating DNA aggregation. Both AFM and zeta potential results support that Mg^{2+} ions induce DNA aggregation. It is possibly due to the reduction of electrostatic repulsion between negatively charged DNA by the presence of Mg^{2+} ion. It should be noted that 10 mM (200 mg/L) Mg^{2+} is within the range of environmentally relevant concentrations determined among soil samples in this study (Table 1).

As described by Shamsi and Kraatz (2013), multi-valent cations such as Mg^{2+} ion tend to bind with DNA more tightly than other monovalent cations. Anastassopoulou and Theophanides (2002) observed that the role of Mg^{2+} ion in DNA stabilization is concentration-dependent. At high concentrations, Mg^{2+} binding induces conformational changes leading to Z-DNA. At low concentrations, it destabilizes DNA in the human body. Similarly, Mg^{2+} at lower concentrations (< 2 mM) is a vital cofactor for enzymatic reactions such as PCR, but Mg^{2+} at higher concentrations (> 5 mM, as was observed for some soil samples), can inhibit PCR (Lim et al., 2017a). It was found that Mg^{2+} ions bind to the phosphate or nitrogen base of DNA and form a super molecular structure, thereby stabilizing DNA structure (Anastassopoulou and Theophanides, 2002). Once DNA is bound with Mg^{2+}, the denaturation of dsDNA can become incomplete during PCR amplification (Theophanides, 1984; Anastassopoulou and Theophanides, 2002). Therefore, it is plausible that the presence of Mg^{2+} ions may hinder DNA hybridization and hence inhibit the NanoGene assay.

In contrast, DNA incubated in the presence of HA did not show any significant DNA aggregation by AFM compared to the control DNA (Fig. 4d and e) and also showed similar zeta potential (49.68 ± 1.41 mV) indicative of dispersed DNA (Table 4). It was expected that some degree of DNA aggregation would occur in the presence of HA due to non-specific binding (adsorption) between DNA and HA as shown in a previous study (Kim et al., 2011a). However, the lack of HA-induced DNA aggregation observed in this study may be due to the difference between the PCR product (~1500 bp) used in this study and gDNA (~4 Mbp) used in the previous study.

DNA incubated together with Mg^{2+} and HA showed significant aggregation along with randomly dispersed HA (shown as dark dots in Fig. 4f, indicated by arrows). The zeta potential results indicate the presence of aggregated DNA when 10 mM Mg^{2+} was present with 0.1 μg/mL (−14.91 ± 4.69 mV) or 0.5 μg/mL HA (−17.20 ± 2.99 mV). This observation indicates that DNA aggregates in the presence of both Mg^{2+} and HA (Tsai and Olson, 1992a, 1992b), but it is the interaction between DNA and Mg^{2+} that is critical for DNA aggregation.

In summary, the major soil properties influencing the NanoGene assay detection of *P. putida* were Mg^{2+} and HA. Most importantly, the Mg^{2+} content of soils strongly influenced the vulnerability of the gene quantification by the NanoGene assay. By identifying the vulnerability of the NanoGene assay to Mg^{2+}, this suggests that incorporation of EDTA or other Mg^{2+} dependent chelator could overcome this inhibitory activity from environmental samples. This can maintain the significant advantage of the NanoGene assay in gene quantification without extensive DNA extraction and purification. These results should enable the NanoGene assay to be used with accuracy and precision even for complex and heterogeneous environmental soils.

Acknowledgement

This study was supported by National Science Foundation (NSF CAREER award #1054768) and National Research Foundation of Korea (NRF-2017005133). The authors appreciate the sampling help of Dr. Joo-Myung Ahn and the donation of marsh sediment samples from Dr. Yucheng Feng at Auburn University.

Appendix A. Supplementary data

Supplementary data related to this article can be found at https://doi.org/10.1016/j.soilbio.2018.08.003.

References

Anastassopoulou, J., Theophanides, T., 2002. Magnesium–DNA interactions and the possible relation of magnesium to carcinogenesis. Irradiation and free radicals. Critical Reviews In Oncology-Hematology 42, 79–91.
ASTM, 1985. Zeta Potential of Colloids in Water and Water Water. ASTM Standard D 4187-82, Conshohocken, PA.
Burt, R., 2004. Soil Survey Laboratory Methods Manual, Soil Survey Investigations Report, Version 4.0 Ed. USDA-NRCS.
Cébron, A., Norini, M.-P., Beguiristain, T., Leyval, C., 2008. Real-time PCR quantification of PAH-ring hydroxylating dioxygenase (PAH-RHD$_\alpha$) genes from Gram positive and Gram negative bacteria in soil and sediment samples. Journal of Microbiological Methods 73, 148–159.
Kim, G.-Y., Son, A., 2010. Development and characterization of a magnetic bead-quantum dot nanoparticles based assay capable of *Escherichia coli* O157:H7 quantification. Analytica Chimica Acta 677, 90–96.
Kim, G.-Y., Wang, X., Ahn, H., Son, A., 2011a. Gene quantification by the NanoGene assay is resistant to inhibition by humic acids. Environmental Science & Technology 45, 8873–8880.
Kim, G.-Y., Wang, X., Son, A., 2011b. Inhibitor resistance and in situ capability of nanoparticle based gene quantification. Journal of Environmental Monitoring 13, 1344–1350.
Lee, E.-H., Chua, B., Son, A., 2015a. Micro corona discharge based cell lysis method suitable for inhibitor resistant bacterial sensing systems. Sensors and Actuators B: Chemical 216, 17–23.
Lee, E.-H., Chua, B., Son, A., 2016. Detection of airborne bacteria with disposable bio-precipitator and NanoGene assay. Biosensors and Bioelectronics 83, 205–212.
Lee, E.-H., Chua, B., Son, A., 2018. Detection of cyanobacteria in eutrophic water using a portable electrocoagulator and NanoGene assay. Environmental Science & Technology 52, 1375–1385.
Lee, E.-H., Lim, H.J., Lee, S.-D., Son, A., 2017. Highly sensitive detection of bisphenol A by NanoAptamer assay with truncated aptamer. ACS Applied Materials & Interfaces 9, 14889–14898.
Lee, E.-H., Lim, H.J., Son, A., Chua, B., 2015b. A disposable bacterial lysis cartridge (BLC) suitable for an in situ water-borne pathogen detection system. The Analyst 140, 7776–7783.
Lim, H.J., Choi, J.-H., Son, A., 2017a. Necessity of purification during bacterial DNA extraction with environmental soils. Environmental Health Toxicology 32, e2017013.
Lim, H.J., Chua, B., Son, A., 2017b. Detection of bisphenol A using palm-size NanoAptamer analyzer. Biosensors and Bioelectronics 94, 10–18.
Mitchell, K.A., Chua, B., Son, A., 2014. Development of first generation in-situ pathogen

detection system (Gen1-IPDS) based on NanoGene assay for near real time *E. coli* O157:H7 detection. Biosensors and Bioelectronics 54, 229–236.
Shacklette, H.T., Boerngen, J.G., 1984. Element Concentrations in Soils and Other Surficial Materials of the Conterminous United States. U.S. Geological survey professional paper 1270.
Shamsi, M.H., Kraatz, H.B., 2013. Interactions of metal ions with DNA and some applications. Journal of Inorganic and Organometallic Polymers and Materials 23, 4–23.
Tebbe, C.C., Vahjen, W., 1993. Interference of humic acids and DNA extracted directly from soil in detection and transformation of recombinant DNA from bacteria and a yeast. Applied and Environmental Microbiology 59, 2657–2665.
Theophanides, T., 1984. Metal ions in biological system. International Journal of Quantum Chemistry 26, 933–941.
Ting, H.-C., Yen, C.-C., Chen, W.-K., Chang, W.-H., Chou, M.-C., Lu, F.-J., 2010. Humic acid enhances the cytotoxic effects of arsenic trioxide on human cervical cancer cells. Environmental Toxicology and Pharmacology 29, 117–125.
Tsai, Y.-L., Olson, B.H., 1992a. Rapid method for separation of bacterial DNA from humic substances in sediments for polymerase chain reaction. Applied and Environmental Microbiology 58, 2292–2295.
Tsai, Y.L., Olson, B.H., 1992b. Detection of low numbers of bacterial cells in soils and sediments by polymerase chain reaction. Applied and Environmental Microbiology 58, 754–757.
Wang, X., Cho, K.-S., Son, A., 2015. Ultrasonication as a rapid and high yield DNA extraction method for bacterial gene quantification by NanoGene assay. Biotechnology and Bioprocess Engineering 20, 1133–1140.
Wang, X., Liles, M.R., Son, A., 2013. Quantification of *E. coli* O157:H7 in soils using an inhibitor-resistant NanoGene assay. Soil Biology and Biochemistry 58, 9–15.